

A Novel Method to Achieve Preferable Bone-to-Implant Contact Area of Zygomatic Implants in Rehabilitation of Severely Atrophied Maxilla

Houzuo Guo,* DMD¹/Xi Jiang,* DMD¹/Ping Di, MD¹/Ye Lin, MD¹

Purpose: To propose and evaluate a novel method for achieving a favorable bone-to-implant contact (BIC) area for zygomatic implants (ZIs). **Materials and Methods:** Patients who needed ZIs to restore a severely atrophied maxilla were recruited. In preoperative virtual planning, an algorithm was utilized to find the ZI trajectory that would achieve the largest BIC area with a predefined entry point on the alveolar ridge. The surgery was conducted according to the preoperative plan with the assistance of real-time navigation. Area BIC (A-BIC), linear BIC (L-BIC), distance from implant to infraorbital margin (DIO), distance from implant to infratemporal fossa (DIT), implant exit section, and deviation of the real-time navigated surgery were measured and compared between the preoperative plan and the placed ZIs. The patients were followed up for 6 months. **Results:** Overall, 11 patients with 21 ZIs were included. The A-BICs and L-BICs were significantly higher in the preoperative plan than in the placed implants ($P < .05$). Meanwhile, there were no significant differences in DIO or DIT. The planned-placed deviation was 2.31 ± 1.26 mm for the entry, 3.41 ± 1.77 mm for the exit, and 3.06 ± 1.68 degrees for the angle. All ZIs survived to the 6-month follow-up. **Conclusion:** This novel method can virtually calculate the trajectory of ZIs and transfer the preoperative plan to surgery to acquire a favorable BIC area. The actual positions of placed ZIs were slightly deviated from the ideal due to navigation errors. *Int J Oral Maxillofac Implants* 2023;38:111–119. doi: 10.11607/jomi.9824

Keywords: accuracy, bone-to-implant contact, maxilla, real-time surgical navigation system, zygomatic implants

Patients with a severely atrophied maxilla pose a challenge for successful rehabilitation with dental implants. Onlay bone grafts, sinus floor elevation, and even vascularized fibular flaps can improve the alveolar conditions to support implants. However, these methods have the limitations of donor site morbidity, multiple surgical interventions, grafting complications, and a long healing period, which pose a burden to both patients and clinicians.¹ Zygomatic implants (ZIs), developed in the early 1990s by Brånemark,² have provided a far simpler approach to restore the atrophic maxilla. ZIs overcome the local osseous defect by engaging with the zygomatic bone, allowing for shortened treatment time, decreased surgical morbidity, and immediate loading.³ Long-term clinical results achieved by ZIs have proven that they are a successful alternative for

rehabilitating severely deficient maxilla.⁴ However, the surgical placement of ZIs is also challenging due to the irregular shape of the zygoma, long trajectory of ZIs, and limited surgical field. Slight deviations of the osteotome may lead to a smaller bone-to-implant contact (BIC) area, which may compromise the implant stability or lead to more serious complications, such as orbital and infratemporal fossa involvement, protrusion of the implant apex, and failed osseointegration.⁵ Thus, the dedicated preoperative planning of ZIs and accurate implementation of the virtual design into surgical reality are crucial.

With the development of real-time navigation systems, implants can be dynamically guided and placed according to the preoperative virtual design.⁶ ZIs that have an apex far away from the oral cavity particularly benefit from using dynamic navigation over static templates.⁷ Recent studies have verified that real-time surgical navigation systems have the advantages of minimizing the risk of intraoperative complications and ensuring stable anchorage during the placement of ZIs.⁸

In preoperative virtual design, the entry point of the ZIs in the alveolar ridge is generally accepted to be in the second premolar or first molar area, within the bone contour of the maxilla.^{9–11} However, the determination of the exit point on the outer surface of the zygoma bone, which then defines the trajectory of the ZI, remains controversial. The optimal exit point would avoid

¹Department of Oral Implantology, Peking University School of Stomatology, Beijing, China.

Correspondence to: Dr Ye Lin; Professor, Department of Oral Implantology, Peking University School of Stomatology, 22 Zhongguancun South Avenue, Haidian District, Beijing 10081, China. Email: yorcklin@263.net

*Houzuo Guo and Xi Jiang contributed equally and should be regarded as co-first authors.

Submitted May 9, 2022; accepted July 15, 2022.

©2023 by Quintessence Publishing Co Inc.

vital anatomic structures and obtain a BIC area as large as possible.⁹⁻¹²

There is no generally accepted method for ZI preoperative planning. Uchida et al⁹ used the jugale (Ju) point, the most depressed point of the transitional region from the lateral margin of the zygomaticofrontal process to the upper margin of the zygomaticotemporal process, as the exit point of ZIs. However, Takamaru et al¹¹ pointed out that the zygomatic bone at the Ju point was too thin to guarantee osseointegration. They recommended that the implant should penetrate at a more inferoanterior position than the Ju point. Wu et al¹³ took the largest internal and external diameters of the zygoma as the exit point, while Pu et al¹⁴ considered the lateral point of the largest coronal area of the maxillary sinus as the points for determining the trajectory of the zygomatic implants. However, these methods cannot precisely provide the best trajectory for each patient.

Thus, the present study aimed to evaluate the clinical feasibility of a novel method based on virtual ZI design via algorithm and a real-time navigation technique to achieve the largest potential BIC area for ZIs in the severely atrophied maxilla.

MATERIALS AND METHODS

Study Design and Subject Enrollment

This prospective clinical study was conducted in the Department of Oral Implantology at Peking University School and Hospital of Stomatology. The trial was approved by the local ethics committee (Institutional Review Board of Peking University School and Hospital of Stomatology [Approval Number: PKUS-SIRB-202166103]) and complied with the tenets of the Declaration of Helsinki. All patients signed a consent form before participation.

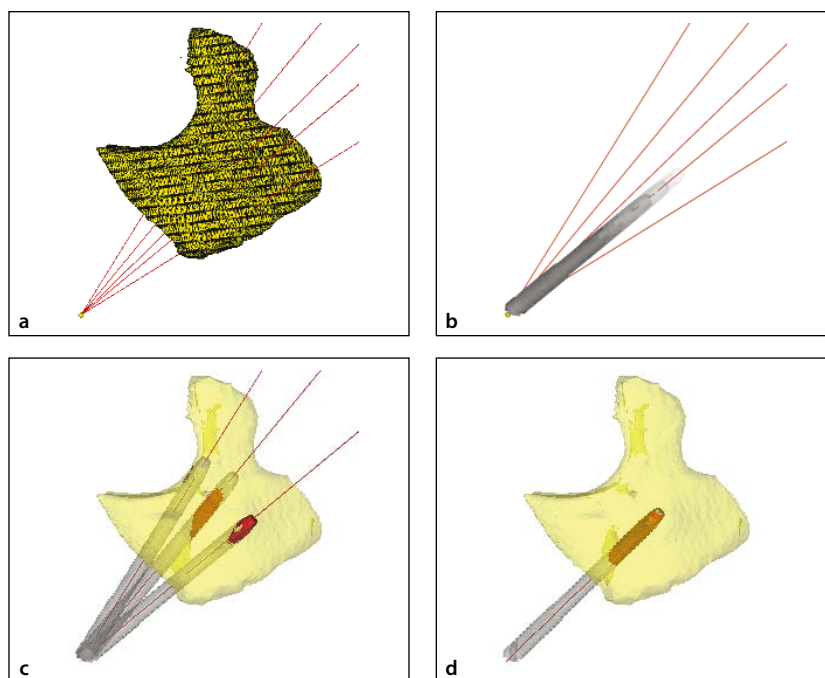
Patients who needed ZIs to restore severely atrophied maxilla were recruited between December 2019 and June 2021. The inclusion criteria were (1) a completely edentulous maxilla or terminal dentition with unsalvageable teeth; (2) sufficient anterior bone height for the placement of two standard implants, along with severe bone loss in the posterior maxilla that prevented the placement of conventional vertical or tilted implants; and (3) full-arch immediate loading requested by the patient. The exclusion criteria were (1) untreated maxillary sinusitis or a maxillary sinus cyst; (2) insufficient bone in the anterior maxilla, thus requiring two ZIs at each side of the maxilla; (3) poor oral hygiene, limited mouth opening, heavy smoking habits (> 20 cigarettes/day), pregnancy, or any history of chemotherapy or radiotherapy; and/or (4) local or systemic contraindications for oral surgery and implant placement.

Preoperative Virtual Design with Algorithm

This study used a preoperative planning software (IVSP Image) with a built-in novel algorithm to find the trajectory of the ZIs with optimal BIC area. The procedure is described as follows:

1. Virtual zygoma bone construction: Prior to planning, four to six miniscrews were placed and adequately distributed in the maxilla for image registration based on the general guidelines of navigation surgery in cases of complete edentulism by West et al.¹⁵ Then, preoperative CBCT (i-CAT FLX, Imaging Sciences International, 120 kVp, 5 mA, 16 × 13 cm) was performed. DICOM data were obtained and imported into the planning software. The virtual zygoma models were created in STL format.
2. Entry point determination: Anatomical landmarks were used to determine the ZI entry point in the oral cavity. The position between the line tangent to the lateral margin of the infraorbital foramen and the zygomaticoalveolar process was selected, which equates to the second premolar or first molar area. Then, a 5 mm palatal shift from the buccal margin of the alveolar ridge was determined as the entry point.⁹⁻¹¹
3. Virtual ZI creation: The virtual ZI models of each length (30, 32.5, 35, 37.5, 40, 42.5, 45, 47.5, 50, and 52.5 mm) were constructed via scanning (3Shape E4) the real ZIs (Brånemark System Zygoma TiUnite, Nobel Biocare) and methods of reverse engineering.
4. Optimal surgical design calculation: After obtaining the virtual zygoma bone model, the coordinates of the corresponding entry point, and the virtual ZI models, the preoperative planning software calculated and determined the length and trajectory of the ZI that would achieve the largest BIC area. The algorithm in the software is based on the enumeration method, and the details are as follows:
 - a. Trajectory enumeration: The facial surface of the STL-formatted zygoma bone was constructed using triangular patches. The coordinate of each vertex of the triangular patch was extracted. The rays, which were made starting from the predefined entry point and crossed each vertex on the facial surface of zygoma bone, represented all possible ZI trajectories (Fig 1a).
 - b. Surgical design enumeration: All possible trajectories starting from the entry point, when combined with all 10 ZI model types (from 35 mm to 52.5 mm, with 2.5-mm intervals), stand for all possible surgical designs (Fig 1b).
 - c. Virtual simulation and design exclusion: All surgical designs were virtually simulated. The designs in which the ZI was less than 1 mm from the orbit or infratemporal fossa or extruding

Fig 1 (a) Trajectory enumeration by connecting the entry point with all vertices on the facial surface of the zygoma bone. (For illustration, the triangles on the zygoma have been reduced). (b) Surgical design enumeration by combining all trajectories with the 10 types of ZI length. (c) Virtual simulations and designs with approximation to the orbit, the infratemporal fossa, or extrusion of more than 0.5 mm out of the facial surface of zygoma were excluded. (d) The simulation with the largest BIC was determined to be the surgical design.



- more than 0.5 mm out of the facial surface of the zygoma were excluded (Fig 1c).
- d. Optimal surgical design determination: An intersectional Boolean operation was performed between the ZI model and the zygoma model in each surgical design. The surface area of the intersectional part was calculated as the value of the BIC area. By enumerating all surgical simulations, the one with the largest BIC area was chosen as the optimal surgical design (Fig 1d).

Transfer of the Preoperative Plan to the Navigation System

In order to accurately implement the ZI surgery according to the preoperative design, the three-dimensional ZI position generated by the planning software needed to be transferred to the navigation system.

In brief, the preoperatively placed fiducial markers (miniscrews) were used to register the preoperative plan in the navigation system (Dcarer Implant Dynamic Navigation, DHC-DI2). Specifically, the ZIs and fiducial markers were exported as an STL file from the planning software, and the STL file and CBCT data were then imported into the navigation system. Lastly, paired-point registration of the markers was used to align the presurgical plan with the CBCT of the patient (Fig 2). After this, the navigation surgery was able to be followed.

Real-Time Navigated Surgery and Postoperative Follow-up

All surgeries were performed under intravenous sedation. Any remaining teeth in the maxilla were extracted. A slight palatal incision and vertical releasing incisions

were performed. The full-thickness flap was elevated to expose the anterolateral wall of the maxillary sinus. The sinus membrane was elevated when the implant went through the sinus, and membrane integration was maintained as much as possible. After image registration according to the fiducial markers, the osteotomy and ZI placement were monitored using a real-time navigation system according to the manual provided by the manufacturer. The navigation tolerance was set at a distance of 0.5 mm and an angle of 2 degrees. Multiunit abutments were connected, and the soft tissue flap was closed. A postoperative CBCT scan was then performed. Immediate restoration was achieved within 24 hours (Fig 3). All patients were given 5-day prescriptions of antibiotics, analgesics, and a mouth rinse solution (chlorhexidine 0.12%).

For postoperative follow-up, all patients with full-arch provisional restorations were routinely revisited to monitor the healing process after 1 week, 1 month, 3 months, and 6 months. Biologic and technical complications were recorded.

Measurements

The preoperative plan and postoperative CBCT data were three-dimensionally superimposed. To facilitate these measurements, the center line and tip of the ZI were manually identified, and the postoperative CBCT scans of the ZIs were replaced with a reverse-engineered virtual implant model. With the centerlines, ZI models, and models of the corresponding zygoma (Fig 4), the following parameters were measured in the graphics processing software (Mimics Research 21.0, Materialise):

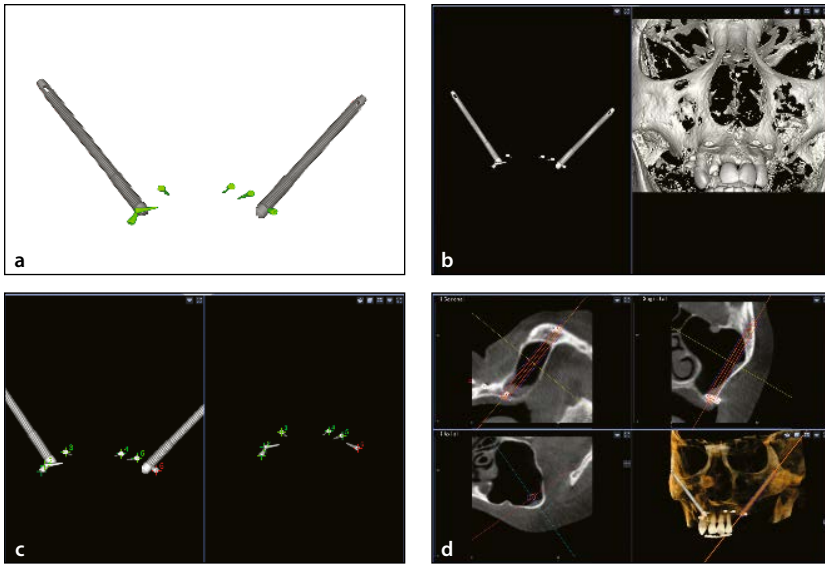


Fig 2 (a) ZIs with the fiducial markers exported as STL file from planning software. (b) Importing the STL file into navigation system. (c) Paired-point registration. (d) Preoperative plan in the navigation system.

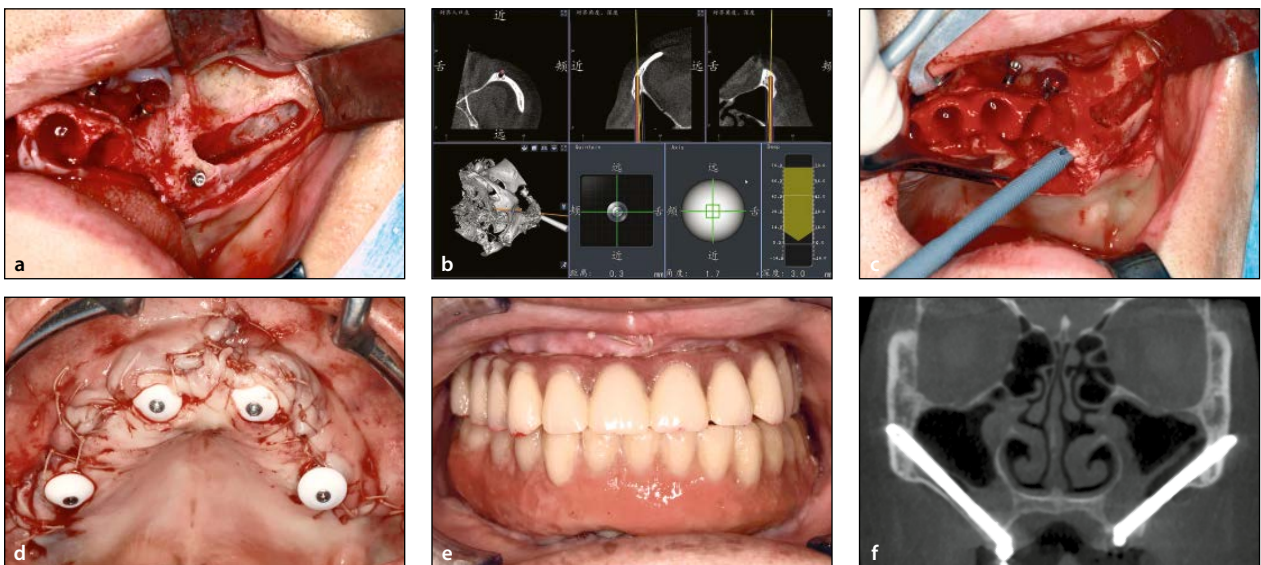


Fig 3 (a) Reflection of the flap and bone window opened for surgical access. (b) Osteotomy under the guidance of the real-time navigation system. (c) ZI insertion. (d) Soft tissue closure with the healing caps placed. (e) Immediate full-arch restoration. (f) Section of the postoperative CBCT scan.

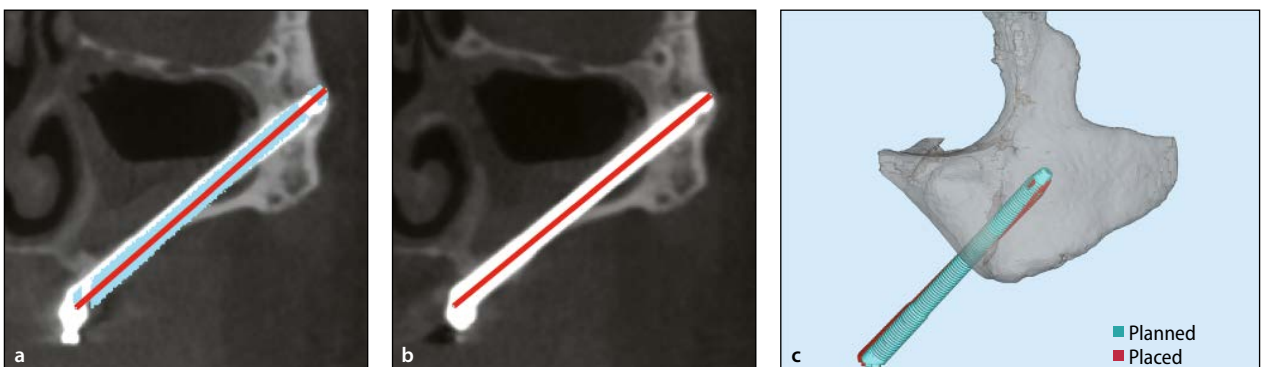
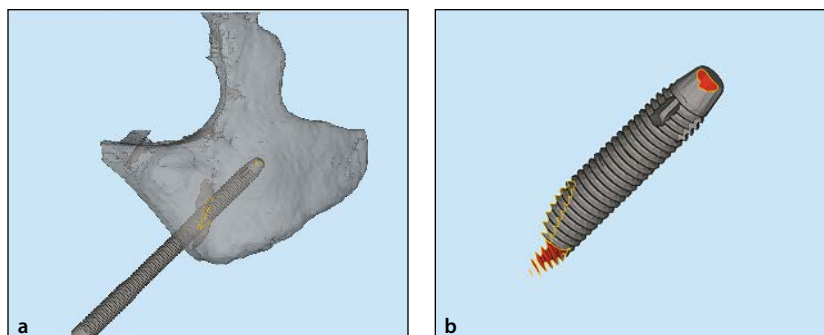


Fig 4 (a) Planned implant and center line. (b) Placed implant and center line, which was then replaced by a virtual ZI model. (c) The virtual models of the zygoma bone, planned ZI, and placed ZI.

Fig 5 (a) Boolean operation to find the intersection between the zygoma and the ZI. (b) The BIC area, as automatically calculated by the software.



- **Area BIC (A-BIC, mm²):** The A-BIC was defined as the surface area of ZI engaged with the zygoma. For the measurements, the intersection of the zygoma and the ZIs were obtained via Boolean operation. The surface areas of both the planned and placed intersections of the zygoma and implant were obtained (Fig 5).
- **Linear BIC (L-BIC, mm):** According to the method proposed by Hung et al,¹⁰ the linear BIC was defined as the average linear value of BIC lengths on the facial and temporal sides of the zygoma in a two-dimensional slice (Fig 6).
- **Implant exit section:** Following the method of Rigolizzo et al,¹⁶ the external surface of the zygomatic bone was divided into 13 sections, as shown in Fig 7. The sections where the exit point of each ZI was located were then recorded.
- **Distance from the implant to the infraorbital margin (DIO, mm) and to the infratemporal fossa (DIT, mm):** The shortest distance from the ZI to the infraorbital margin was recorded as the DIO. The shortest distance from the ZI to the infratemporal fossa was recorded as the DIT. If the implant entered the orbit or infratemporal fossa, the value was recorded as 0 mm.
- **Deviation of the real-time navigated surgery:** Discrepancies between the planned and placed implants. **Entry deviation (mm):** distance between the entry points. **Exit deviation (mm):** distance between the exit points. **Angular deviation (degrees):** angle of long axes (Fig 8).

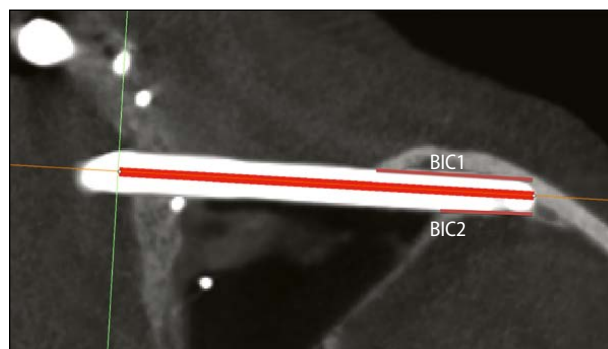


Fig 6 Linear BIC measurement of the ZI in two dimensions.

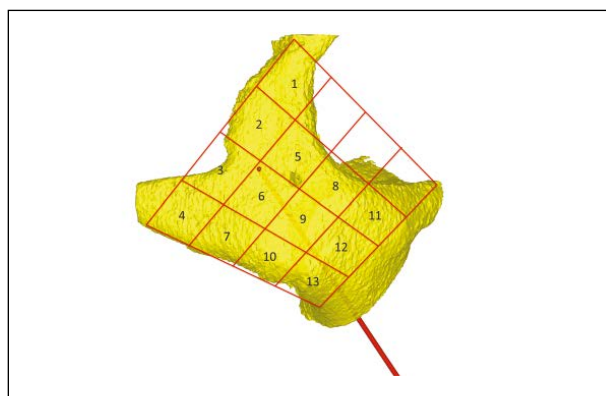


Fig 7 The facial surface of the zygoma was manually divided into 13 sections to record the exit position of ZI.

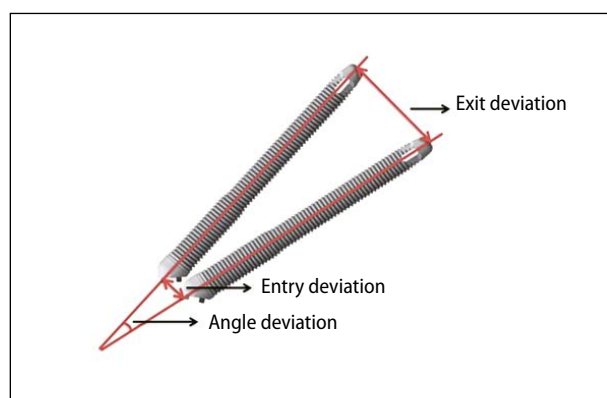


Fig 8 Schematic illustration of the deviations.

Statistical Analysis

The A-BIC, L-BIC, DIO, and DIT were described as mean and SD values, then compared between the planned and placed ZIs. Normally distributed values were compared using paired *t* test, while nonnormally distributed values were analyzed using Wilcoxon signed rank test. The percentages of the planned and placed ZI exit sections were counted, and the deviations of the real-time navigated implant surgery were recorded. All statistical analyses were performed using SPSS version 24.0. A *P* value of < .05 was considered significant.

Table 1 Demographic and Medical Characteristics of the Recruited Patients

Characteristics	
Gender	
Men	6
Women	5
Age (y)	
Mean	56
Range	44–71
Maxillary status	
Completely edentulous	4
Potentially edentulous	7
ZI length (mm)	
35	2
40	5
42.5	2
45	4
47.5	2
50	3
52.5	3

Table 2 Parameters of the Planned and Placed Implant Groups

Parameters	Planned implant	Placed implant	P value
A-BIC (mm ²)	242.55 ± 79.08 (153.55–406.03)	210.30 ± 82.34 (90.65–404.75)	.000***
L-BIC (mm)	16.73 ± 4.61 (11.13–26.41)	15.17 ± 4.67 (8.94–26.84)	.006**
DIO (mm)	8.74 ± 5.42 (1.04–18.35)	10.31 ± 3.58 (2.52–16.19)	.108
DIT (mm)	1.28 ± 0.33 (0.94–1.60)	1.36 ± 1.00 (0.24–3.35)	.737

Values are presented as mean ± SD (range).

***P* < .01.

****P* < .001.

Table 3 Percentage of the Implant Exit Section

Section	Planned implant	Placed implant
10	4.76	4.76
9	42.86	47.62
8	9.52	9.52
6	14.29	9.52
5	28.57	28.57

Table 4 Total Mean ± SD Deviations of the Real-Time Navigated Surgery (mm)

Entry deviation	Exit deviation	Angle deviation
2.31 ± 1.26	3.41 ± 1.77	3.06 ± 1.68

RESULTS

A total of 11 eligible patients (7 terminal dentition and 4 completely edentulous patients) were recruited, and 21 ZIs were placed according to the aforementioned protocol. The clinicodemographic characteristics of the patients are summarized in Table 1. All ZIs survived to the end of the 6-month follow-up period. At 3 to 6 months postoperation, 2 patients developed a fracture of the temporary acrylic prosthesis, and another participant experienced loosening of the abutment screws. The provisional prostheses were repaired, and the loosening screws were retightened. The healing process was uneventful. All 11 patients received definitive prostheses at 6 months postoperation.

The values of A-BIC were $242.55 \pm 79.08 \text{ mm}^3$ for the planned implant and $210.30 \pm 82.34 \text{ mm}^3$ for the placed implant, while the L-BIC were $16.73 \pm 4.61 \text{ mm}$ and $15.17 \pm 4.67 \text{ mm}$, respectively. Significant differences were found between these two parameters ($P < .05$). The DIO and DIT were $8.74 \pm 5.42 \text{ mm}$ and $1.28 \pm 0.33 \text{ mm}$ in the planned implants and $10.31 \pm 3.58 \text{ mm}$ and $1.36 \pm 1.00 \text{ mm}$ in the placed implants, respectively. No significant differences were found ($P > .05$; Table 2).

Section 9 was the most frequently exited section in the planned (42.86%) and placed (47.62%) ZIs. (Table 3)

Comparing the preoperative plan with the navigated placed implant, the mean entry deviation was $2.31 \pm 1.26 \text{ mm}$, the exit deviation was $3.41 \pm 1.77 \text{ mm}$, and the angular deviation was $3.06 \pm 1.68 \text{ degrees}$ (Table 4).

DISCUSSION

ZIs overcome the limitations of the standard methods of rehabilitating severely atrophied maxillae, but they are challenging to place surgically, and current methods cannot accurately find the optimal trajectory for individual patients. This study proposed a novel method to facilitate ZIs by achieving preferable BIC area. The results showed that with the new preoperative planning method and the assistance of a real-time navigation system, all ZIs gained reliable BIC and survived to the end of the 6-month follow-up period.

Zygomas have a unique shape, and the thickness and length of the zygoma vary between individuals. Accordingly, efforts have been made to detect the most promising region for the placement of ZIs. CBCT and cadaver studies found that zygomas are thickest in sections 5, 8, and 9, and this is where the ZI should be placed.^{10,16} The results of the present study were consistent with those findings. The exit section of the planned and placed ZIs did not differ due to the use of real-time navigation. Two-thirds of the ZIs penetrated at the center and

posterosuperior regions, corresponding to sections 5 and 9. However, one-third of ZIs in the present study obtained the largest BICs in a section other than the center or posterosuperior region. This means that the traditional methods of choosing the ZI trajectory, which are based on certain penetrating regions or locations of the zygoma, might miss the optimal plan due to individualized zygoma anatomy. With the advantages of digital techniques, a computer algorithm based on enumeration was used to determine the optimal ZI position in the present study. With certain prerequisites, all of the possible designs, with different trajectories and implant lengths, were virtually simulated, and the BIC areas were calculated. The exclusive design with the largest BIC area was chosen as the preoperative plan. This approach can theoretically acquire the optimal ZI position even when considering the anatomical variations of different zygomas. To the best knowledge of the authors, this has not yet been reported.

BIC has been established as an important factor that influences the initial and long-term stability of implants. Linear BIC measurements of ZIs in two dimensions have been reported in previous studies. In a study of 77 patients with 173 ZIs by Balshi et al,¹⁷ the average L-BIC was 15.3 mm. Wanget al⁸ reported an L-BIC of 14.9 ± 3.7 mm in 4 patients with 8 implants. In the present study, the L-BIC of 21 ZIs reached 15.17 ± 4.67 mm, which is not obviously better than the results in the previous studies. This might be explained by ethnic differences. Previous studies have demonstrated morphologic zygomatic differences between various ethnic groups.¹⁸ High cheek bones, or a projecting zygoma, which imply a more curved zygomatic bone and a correspondingly short zygoma penetration distance, are strongly associated with Asian people.¹⁹ These ethnic differences might be a possible explanation for why the present L-BIC results were not better than those of previous studies, which did not use any planning algorithms. The L-BIC of the planned ZIs was 16.72 ± 4.61 mm, which was significantly higher than that of the placed implant. This deviation might have been caused by the navigation process. The adequate L-BIC values for successful osseointegration and immediate loading of ZIs are still unclear.⁸

The L-BIC was acquired in a two-dimensional slice, which might be inaccurate for representing the actual surface area embedded in the zygoma bone.²⁰ In this study, the BIC area could be easily measured using volumetric imaging software. The planned and placed BIC areas were 242.55 ± 79.08 mm² and 210.30 ± 82.34 mm², respectively. This discrepancy may also be attributed to deviations that occurred during the navigated steps. The A-BIC, calculated from three-dimensional data, seems to be more reasonable than the two-dimensional linear measurement. However, this parameter has not yet been reported in the literature.

DIO and DIT are two parameters related to the safety of ZIs. The DIOs in the present study, 8.74 ± 5.42 mm in the virtual plan and $10.31 \text{ mm} \pm 3.58$ mm in the placed ZIs, were adequately safe to avoid any orbit engagement. The DITs were 1.28 ± 0.33 mm and 1.36 ± 1.00 mm in the planned and placed ZIs, respectively, which indicated that ZIs were generally close to the infratemporal fossa. This may be due to the nature of the zygomatic anatomy. The thickness of the zygoma near the infratemporal fossa gradually decreases to a range of only 1.8 to 6.1 mm.¹¹ In addition, the apical diameter of the ZI is approximately 2.5 mm, which makes the tip of the implant easy to be near—or even enter—the infratemporal fossa, especially when the implant angle is too low or the implant length is too long.⁹ In the present study, two ZIs partially penetrated the infratemporal fossa, but no serious complications were observed. There have been no reports of serious complications caused by ZIs penetrating the infratemporal fossa. Some authors have even suggested that ZIs could partially intrude into the infratemporal fossa and then penetrate through the zygomatic arch to obtain more cortical bone anchorage.²¹ However, drilling into the temporal fossa increases the risk of bleeding and hematoma, which have been categorized as intraoperative complications by many works in the literature.^{9,10,22}

Deviations in the navigated surgery can be caused by many factors, including technical error, registration error, application error, and human error.²³ The total deviation can be measured by combining preoperative and postoperative CBCT images. The results of navigated deviations in the present study demonstrated an entry deviation of 2.31 ± 1.26 mm, an exit deviation of 3.41 ± 1.77 mm, and an angular deviation of 3.05 ± 1.68 degrees. These values appear to be generally larger than previously reported deviations, such as those by Hung et al⁷ in 2017 (entry deviation = 1.35 ± 0.75 mm; exit deviation = 2.15 ± 0.95 mm; and angular deviation = 2.05 ± 1.02 degrees), Hung et al²⁴ in 2016 (entry deviation = 1.07 ± 0.15 mm; exit deviation = 1.20 ± 0.46 mm; and angular deviation = 1.37 ± 0.91 degrees), and Xiaojun et al²⁵ in 2009 (entry deviation = 1.36 ± 0.59 mm; exit deviation = 1.57 ± 0.59 mm; and angular deviation = 4.10 ± 0.90 degrees). This may be due to differences in navigation systems or surgeon experience with these systems. The deviations in the navigated surgery may be a main factor leading to a lower placed BIC than planned BIC in the present study.

Immediate full-arch loading is one of the most significant advantages of ZIs over traditional methods, such as sinus grafting or short implants, in rehabilitating severely resorbed maxillae.³ Insufficient initial stability impedes the immediate restoration of ZIs, which could also prevent the uneventful osseointegration of ZIs. A systematic review reported that the majority of failed

ZIs occur during the 6-month osseointegration phase.²⁶ In the present study, all 21 ZIs were immediately loaded due to favorable primary stability and survived to the 6-month follow-up. The novel approach of virtual planning using an algorithm and real-time navigation system might contribute to the short-term success. However, it is important to remember that rehabilitation with ZIs requires more than just initial stability and adequate BIC. Meticulous pretreatment evaluation, thorough exploration of local anatomy, surgeon experience, and patient hygiene ability are all critical to the long-term success of ZIs.

This study proposed a new preoperative plan algorithm that could theoretically determine the best ZI trajectory for individualized patient treatment, considering the implant-zygoma bone contact area. The virtual design was then realized using a real-time implant-navigation system. The feasibility of this approach was preliminarily evaluated based on clinical and radiographic outcomes. However, there are some limitations of this study: (1) a short follow-up time of only 6 months, despite the fact that long-term results are required to reliably assess the predictability of the technique; (2) the lack of a control group to determine whether this method is superior to traditional methods; and (3) a relatively small number of participants, which is not sufficient to provide convincing evidence. Further studies are needed to verify this technique.

CONCLUSIONS

This novel virtual planning algorithm can find the potential optimal trajectory for ZIs during preoperative planning. A real-time navigation system facilitates transference of the plan and acquisition of a preferable BIC area in real surgery. The actual positions of the placed ZIs were slightly deviated from the ideal due to navigation errors.

ACKNOWLEDGMENTS

The authors thank Mr. Qiang Hao, the dental technician from the Department of Oral Implantology at Peking University School and Hospital of Stomatology in Beijing, for his support in achieving techniques and materials. The authors wish to express their sincere gratitude to Ms Yachi Zhang, Huitao Wang, and Jing Li from the Department of Oral Implantology at Peking University School and Hospital of Stomatology in Beijing for coordination and support during the study. The authors declare no conflicts of interest. Author contributions: Houzuo Guo: Conceptualization (equal), data curation (lead), formal analysis (lead), methodology (lead), writing – original draft (lead). Xi Jiang: Conceptualization (equal), data curation (equal), investigation (equal), methodology (equal), resources (equal), supervision (equal), writing – review and editing (lead). Ping Di: Data curation (supporting), investigation (supporting), resources

(supporting), supervision (supporting). Ye Lin: Conceptualization (equal), methodology (equal), resources (lead), supervision (lead), writing – review and editing (lead). Data availability: The data that support the findings of this study are available from the corresponding author upon reasonable request. Funding: Research fund for the healthcare of the central committee, “Application of digital technology in immediate implant after tooth extraction” (2022ZD18).

REFERENCES

1. Aparicio C, Manresa C, Francisco K, et al. Zygomatic implants: Indications, techniques and outcomes, and the zygomatic success code. *Periodontol* 2000 2014;66:41–58.
2. Brånemark PI, Gröndahl K, Öhrnell LO, et al. Zygoma fixture in the management of advanced atrophy of the maxilla: Technique and long-term results. *Scand J Plast Reconstr Surg Hand Surg* 2004;38:70–85.
3. Wu Y, Wang F, Huang W, Fan S. Real-time navigation in zygomatic implant placement: Workflow. *Oral Maxillofac Surg Clin North Am* 2019;31:357–367.
4. Goiato MC, Pellizzer EP, Moreno A, et al. Implants in the zygomatic bone for maxillary prosthetic rehabilitation: A systematic review. *Int J Oral Maxillofac Surg* 2014;43:748–757.
5. Bedrossian E, Bedrossian EA. Prevention and the management of complications using the zygoma implant: A review and clinical experiences. *Int J Oral Maxillofac Implants* 2018;33:e135–e145.
6. Schramm A, Gellrich NC, Schimming R, Schmelzeisen R. Computer-assisted insertion of zygomatic implants (Brånemark system) after extensive tumor surgery [in German]. *Mund Kiefer Gesichtschir* 2000;4:292–295.
7. Hung KF, Wang F, Wang HW, Zhou WJ, Huang W, Wu YQ. Accuracy of a real-time surgical navigation system for the placement of quad zygomatic implants in the severe atrophic maxilla: A pilot clinical study. *Clin Implant Dent Relat Res* 2017;19:458–465.
8. Wang F, Bornstein MM, Hung K, et al. Application of real-time surgical navigation for zygomatic implant insertion in patients with severely atrophic maxilla. *J Oral Maxillofac Surg* 2018;76:80–87.
9. Uchida Y, Goto M, Katsuki T, Akiyoshi T. Measurement of the maxilla and zygoma as an aid in installing zygomatic implants. *J Oral Maxillofac Surg* 2001;59:1193–1198.
10. Hung KF, Ai QY, Fan SC, Wang F, Huang W, Wu YQ. Measurement of the zygomatic region for the optimal placement of quad zygomatic implants. *Clin Implant Dent Relat Res* 2017;19:841–848.
11. Takamaru N, Nagai H, Ohe G, et al. Measurement of the zygomatic bone and pilot hole technique for safer insertion of zygomatic implants. *Int J Oral Maxillofac Surg* 2016;45:104–109.
12. Rossi M, Duarte LR, Mendonça R, Fernandes A. Anatomical bases for the insertion of zygomatic implants. *Clin Implant Dent Relat Res* 2008;10:271–275.
13. Wu YQ, Zhang ZY, Zhang CP, Huang W, Sun J, Zhang ZY. The installation of zygomatic implants and drilling guide [in Chinese]. *Zhonghua Kou Qiang Yi Xue Za Zhi* 2006;41:140–143.
14. Pu LF, Tang CB, Shi WB, et al. Age-related changes in anatomic bases for the insertion of zygomatic implants. *Int J Oral Maxillofac Surg* 2014;43:1367–1372.
15. West JB, Fitzpatrick JM, Toms SA, Maurer CR Jr, Maciunas RJ. Fiducial point placement and the accuracy of point-based, rigid body registration. *Neurosurgery* 2001;48:810–817.
16. Rigolizzo MB, Camilli JA, Francischone CE, Padovani CR, Brånemark PI. Zygomatic bone: Anatomic bases for osseointegrated implant anchorage. *Int J Oral Maxillofac Implants* 2005;20:441–447.
17. Balshi TJ, Wolfinger GJ, Shuscavage NJ, Balshi SF. Zygomatic bone-to-implant contact in 77 patients with partially or completely edentulous maxillas. *J Oral Maxillofac Surg* 2012;70:2065–2069.
18. Oetlé AC, Demeter FP, L’Abbé E N. Ancestral variations in the shape and size of the zygoma. *Anat Rec* 2017;300:196–208.
19. Chen T, Hsu Y, Li J, et al. Correction of zygoma and zygomatic arch protrusion in East Asian individuals. *Oral Surg Oral Med Oral Pathol Oral Radiol Endod* 2011;112:307–314.

20. Bertos Quílez J, Guijarro-Martínez R, Aboul-Hosn Centenero S, Hernández-Alfaro F. Virtual quad zygoma implant placement using cone beam computed tomography: Sufficiency of malar bone volume, intraosseous implant length, and relationship to the sinus according to the degree of alveolar bone atrophy. *Int J Oral Maxillofac Surg* 2018;47:252–261.
21. Jensen OT, Brown C, Blacker J. Nasofacial prostheses supported by osseointegrated implants. *Int J Oral Maxillofac Implants* 1992;7:203–211.
22. Chrcanovic BR, Oliveira DR, Custódio AL. Accuracy evaluation of computed tomography-derived stereolithographic surgical guides in zygomatic implant placement in human cadavers. *J Oral Implantol* 2010;36:345–355.
23. Widmann G, Stoffner R, Bale R. Errors and error management in image-guided craniomaxillofacial surgery. *Oral Surg Oral Med Oral Pathol Oral Radiol Endod* 2009;107:701–715.
24. Hung K, Huang W, Wang F, Wu Y. Real-time surgical navigation system for the placement of zygomatic implants with severe bone deficiency. *Int J Oral Maxillofac Implants* 2016;31:1444–1449.
25. Xiaojun C, Ming Y, Yanping L, Yiqun W, Chengtao W. Image guided oral implantology and its application in the placement of zygoma implants. *Comput Methods Programs Biomed* 2009;93:162–173.
26. Chrcanovic BR, Abreu MH. Survival and complications of zygomatic implants: A systematic review. *Oral Maxillofac Surg* 2013;17:81–93.